

See discussions, stats, and author profiles for this publication at: <https://www.researchgate.net/publication/267212736>

Preprocessing EO-1 Hyperion hyperspectral data applied to forests and vegetation classification

Conference Paper · November 2014

CITATION

1

READS

1,266

3 authors:



Youcef Smara

University of Science and Technology Houari Boumediene (USTHB)

93 PUBLICATIONS 123 CITATIONS

[SEE PROFILE](#)



Zohra Hamadache

University of Science and Technology Houari Boumediene

13 PUBLICATIONS 35 CITATIONS

[SEE PROFILE](#)



Seloua Chouaf

University of Science and Technology Houari Boumediene

8 PUBLICATIONS 2 CITATIONS

[SEE PROFILE](#)

Some of the authors of this publication are also working on these related projects:



Speckle Filtering In Polarimetric Radar SAR Images [View project](#)



study of the desertification in semi aride regions of Algeria using satellite data. [View project](#)

Preprocessing EO-1 Hyperion Hyperspectral Data to Support the Application of Forests and Vegetation Classification

AUTHORS:

Zohra HAMADACHE, Youcef SMARA & Seloua CHOUAF

AFFILIATIONS:

Laboratory of Image Processing and radiation. Faculty of Electronics and Computer Science.
University of Sciences and Technology Houari Boumediene (USTHB).
BP 32, El-Alia, Bab-Ezzouar, 16111 Algiers, Algeria.
phone: 213 21 24 79 12 / 806, fax: 213 21 24 71 87,
email: zhamadache.edtas@gmail.com and yousmara@yahoo.com

ABSTRACT

Contrary to the airborne hyperspectral data, the SNR (Signal-to-Noise Ratio) of the spaceborne hyperspectral data of the Hyperion instrument falls from 500 to 50 and Hyperion data are affected by the striping effect related to a small relative errors calibration of each detector caused by the pushbroom technology, which need to be corrected in order to get a better image analysis and interpretation of Hyperion data.

In this study, Hyperion Level 0 (raw, uncalibrated) (Data file name: EO1H0460282009231110KF: EO12009231_7FED7FEC_r1_PF2_01.L0) data of Mt. St. Helens (USA) site provided by the EO-1 Mission, NASA/USGS was used. This image was acquired in August 19, 2009, it has width 256 cross-track samples, 242 spectral channels. The Hyperion imager produces 12-bit data samples. In the file here, each sample is stored as a 2-byte unsigned integer in little-endian byte order, samples arranged in BIP order. In order to correct vertical stripes in Hyperion data, we studied and tested two methods compared to the one implemented by ENVI. Thereafter, we applied ENVI QUAC (QUick Atmospheric Correction) tool to obtain reflectance data.

This preprocessing followed by spectral features analysis and a supervised classification to see whether the data were preserved or disturbed after striping noise reduction. To ensure the reliability of our classification, we used two methods of data reduction which are the PCA (Principal Components Analysis) of ENVI software and the developed unidimensional wavelet transform applied on the data.

Hyperion image has 242 spectral bands in the wavelength range of 0.4 to 2.5 μm . This image has a 10-nm spectral resolution and a 30-m spatial resolution. The destriping algorithms have been adopted to the 242 spectral channels.

KEYWORDS:

Hyperion, Striping effect, Hyperspectral, Classification, Spectral Analysis, PCA, Wavelet transform.

1. INTRODUCTION

The effect known as “striping” was visually obvious in all Hyperion data. If one detector of an array (in either the VNIR or SWIR arrays) has a slightly modified or unbalanced responsivity from that of its neighbours or from its normal condition, the result is a vertical “stripe” in the corresponding band of the image data. If the difference of this response is persistent, the effect can be reduced or eliminated by “fine tuning” the calibrations which are normally different for each detector array. [8] The stripes are present in most channels to some degree but are often pronounced in the SWIR and in channels with low SNR. [9] Data of extreme bands (bands which contain little or no valid data) are identified as “bad” pixels and each column in a single band corresponds to a single detector in one of the arrays. Correlated blocks of stripes seem more prevalent in the SWIR than the VNIR. [3] Since the data are generated from separate detector arrays, which utilise different detector materials, the striping effects had different characteristics in the VNIR and SWIR arrays. [8] To reduce the striping effect, several methods exist in the literature such those based on statistics-based algorithm and those based on spectral filtering. This paper focus on the “local” and “global” approaches, these approaches statistically balance the columns by applying image-based mean and standard deviation values [3] as well as the “destriping based on ENVI SPEAR Tools- Vertical Stripe Removal” [7]. The algorithms of the “local” and “global” approaches in this paper have been provided as an IDL script. The goal of this study is the correction of the striping effect in order to be able to exploit the hyperspectral data in an optimal way, because vertical stripes will lead to faulty interpretation results of the data. Therefore, a striping noise reduction algorithm that provides optimal results in both the elimination of the vertical stripes in the image and the preservation of the original spectral information should be applied. Thus, it will be a question of developing the adopted approaches, of testing and comparing them as an important part of the Hyperion processing.

2. HYPERION IMAGE PREPROCESSING FLOWCHART

The purpose of the destriping process is to reduce or remove the vertical stripes in Hyperion data without disturbing the spectral information. The destriping and evaluation flowchart of Hyperion data is shown in (Fig. 1).

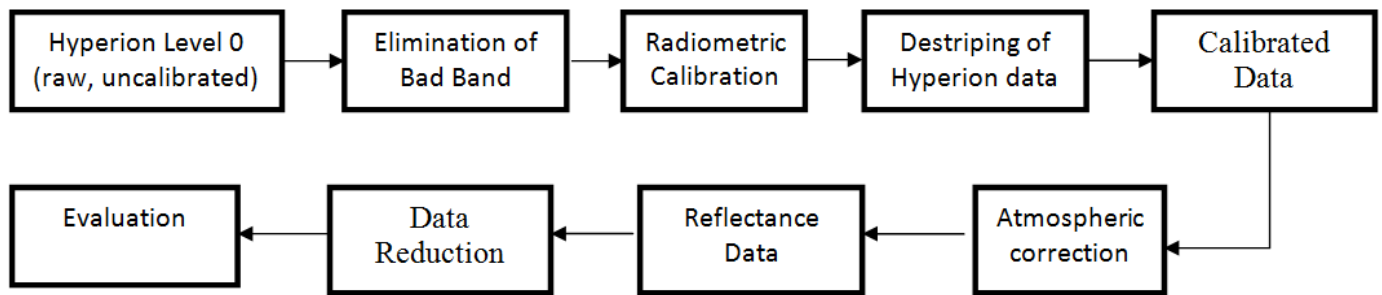


Fig. 1: Hyperion image preprocessing flowchart

2.1. Elimination of bad bands

The Hyperion dataset are not immune to the effects of the intervening atmosphere and water vapor absorption which cause a low SNR in some bands. In addition, some of the bands belonging to two spectrometer datasets in the VNIR the SWIR regions overlap. Based on the above, only 153 of the 242 total bands were selected for spectral features analysis. These bands are: 8 to 57, 79 to 97, 101 to 119, 134 to 164, 183 to 184 and 187 to 218.

2.2. Radiometric calibration

In pushbroom sensors such as Hyperion instrument, striping noise is caused by the non-perfect calibration which causes a vertical stripes where the DN (Digital Numbers) values in the stripe were consistently lower than those in the adjacent columns. In this study, the global and local approaches compared to the destriping based on ENVI-SPEAR-Tools – Vertical Stripe Removal were used to repair the vertical striping.

2.3. Atmospheric correction using QUAC (ENVI)

In order to convert the Hyperion image from radiance to reflectance data, the atmospheric correction used here in this study was made by using the tool named QUAC (QUick Atmospheric Correction) of ENVI software to achieve atmospheric correction of images.

2.4. Evaluation

The evaluation of the destriping methods was done using a spectral analysis and two methods of data reduction which are PCA of ENVI software and the developed unidimensional wavelet transform followed by a supervised classification.

3. STRIPING NOISE REDUCTION IN HYPERION DATA

In the pushbroom Hyperion sensor, the striping noise is an effect perceived such as columns in the vertical direction, visually apparent and pronounced well in almost all bands of Hyperion. An ideal destriping method should be able to eliminate the stripes without altering the information of the original image, and pixels values not affected by stripes should not be changed after destriping process to preserve the original data. Several methods were proposed such as histogram matching [18] and spectral filtering [15]. Gadallah *et al.* [5] suggested matching the gain and offset of each sensor to typical values, Chander *et al.* [2] used an inverse regression to reduce striping in Landsat TM band-6 data. On the other side, Nishii *et al.* [12] applied univariate Bayesian regressions for spatial smoothing. Another method was developed to destripe EO-1 Hyperion hyperspectral imagery locally or globally [3]. Moreover, spectral model was also constructed to correct airborne imaging spectrometer data [4]. A similar algorithm was modified to deal with the spaceborne EO-1 Hyperion data [10].

These algorithms involved in adjusting gray values column by column or line by line for all spectral bands according to a calculated offset relative to the average of the entire scene, thus also requiring thorough scene examination and intensive computation. [17] The spectral filtering was also used to reduce striping noise [1], Fast Fourier transform (FFT)-based semiautomatic filtering was also used to eliminate striping patterns in Landsat-7 Enhanced TM plus image pairs for better imageodesy analysis [11], wavelet analysis [16] and spline interpolation [17]. Among the ideas proposed, the simplest is statistical balancing using the means or the means and variances of the columns of the data image. A vertical stripe is said to occur where the statistics indicate that the image information is likely to be valid (that is, the pixel is not “bad”) but with significantly modified gain and offset. In addition to assuming the data are valid, we are also assuming that such gains and offsets are relatively stable over a collect, but not necessarily between collects. A general approach to removing vertical stripes with these characteristics is then similar to methods used in the past to balance horizontal stripes in mirror scanner images by histogram equalization (Horn and Woodham, 1979) [7] or to flatten images affected by limb brightening or to balance detectors in airborne pushbroom sensors

(Goetz et al. 1985) [6]. That is, histogram moments, such as the means and variances of the columns in each band, are used to balance the statistics of the arrays to those of a reference histogram. [3]

4. METHODOLOGY

In order to correct vertical striping in the image, the destriping algorithms developed in this study are:

3.1. The global approach based on a method by Datt et al. (2003) [3]

In global balancing, the statistical moments of each column are modified to match those for the whole image for each band.

Mathematically, let m_{ik} be the mean of the detector at the i 'th pixel position for band k and S_{ik} be the corresponding within-column standard deviation over the data sensed as the image is acquired – or on some group of lines in the image. Moreover, let \bar{m}_{ik} and \bar{S}_{ik} be corresponding “reference” values for these moments. The differences between local and global methods and the outlier or general image passes occur in the way the reference values are established.

Formally, the approaches (global and local) can all be expressed as finding a gain (α_{ik}) and an offset (β_{ik}) for each detector such that the values of the image data for sample i , line j and band k (x_{ijk}) are modified to:

$$x'_{ijk} = \alpha_{ik}x_{ijk} + \beta_{ik} \quad \dots (1)$$

where the gain and offset are computed by:

$$\alpha_{ik} = \frac{\bar{S}_{ik}}{S_{ik}} \quad \dots (2)$$

$$\beta_{ik} = \bar{m}_{ik} - \alpha_{ik}m_{ik} \quad \dots (3)$$

The global method takes the reference mean to be the total image mean and may also take the reference standard deviation to be the whole image within-column standard deviation:

$$\bar{m}_{ik} = \bar{m}_k \quad \dots (4)$$

$$\bar{S}_{ik} = \bar{S}_k \quad \dots (5)$$

The global approach is based on the applying of the mean and standard deviation values of each band to the entire band. [13]

3.2. The local approach based on a method by Datt et al. (2003) [3]

In the local approach, reference moments are estimated locally. However, if an affected pixel is extreme but not “bad”, its presence can adversely affect the local statistics. It is best to treat these outliers separately in an initial pass. The initial outlier pass used here is local but uses median statistics rather than means and identifies the pixels to adjust from set thresholds rather than modifying all of the column data. The local methods involve either outlier detection and replacement or the use of local smoothing filters. For outlier detection (assuming “bad” pixels have been previously fixed) it is possible to compute:

$$test = \frac{|m_{ik} - l_{med}(m_{ik})|}{l_{med}(S_{ik})} \quad \dots (6)$$

where “ l_{med} ” indicates a local median of selectable neighborhood. Outlier pixels are those where “test” is above a specified threshold. Pixels with anomalous standard deviations are also identified by a similar formula. The outlier de-striping is applied as an initial pass to the identified bands using median values as the reference values.

Local “de-striping” proceeds when the outliers have been treated. It uses as reference values:

$$\bar{m}_{ik} = l_{mean}(m_{ik}) \quad \dots (7)$$

$$\bar{S}_{ik} = l_{mean}(S_{ik}) \quad \dots (8)$$

The notation “ l_{mean} ” used here indicates a local mean with selectable neighborhood.

The local approach is based on the applying of the mean and standard deviation values around them to the bad columns, the columns are statistically balanced. [13]

3.3. Destriping based on ENVI-SPEAR-Tools – Vertical Stripe Removal [14]

This method is also implemented in ENVI but only inadequately described in publications or manuals. However, an advantage may be the option to exclude certain areas from the corrections, e.g. very bright (mostly clouds) or very dark image areas.

5. EXPERIMENTAL RESULTS

Destriping results on the Mont Saint Helens (USA) images of the Hyperion sensor:

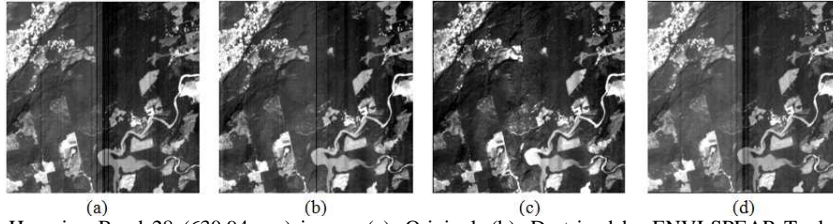


Fig.2: Destriping results of the Hyperion Band 28 (630.94 nm) image. (a): Original. (b): Destriped by ENVI-SPEAR-Tools – Vertical Stripe Removal. (c): Destriped by the global approach. (d): Destriped by the local approach

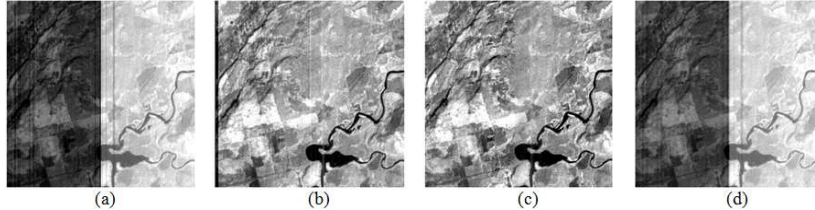


Fig.3: Destriping results of the Hyperion Band 57 (925.85 nm) image. (a): Original. (b): Destriped by ENVI-SPEAR-Tools – Vertical Stripe Removal. (c): Destriped by the global approach. (d): Destriped by the local approach

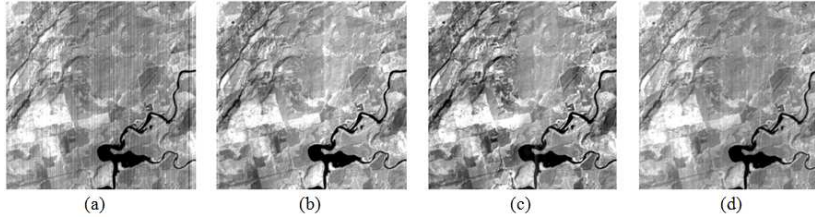


Fig.4: Destriping results of the Hyperion Band 90 (1043.67 nm) image. (a): Original. (b): Destriped by ENVI-SPEAR-Tools – Vertical Stripe Removal. (c): Destriped by the global approach. (d): Destriped by the local approach

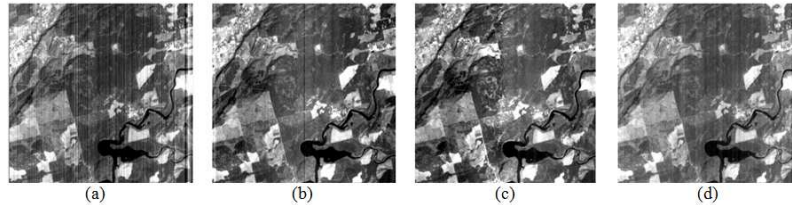


Fig.5: Destriping results of the Hyperion Band 160 (1749.85 nm) image. (a): Original. (b): Destriped by ENVI-SPEAR-Tools – Vertical Stripe Removal. (c): Destriped by the global approach. (d): Destriped by the local approach

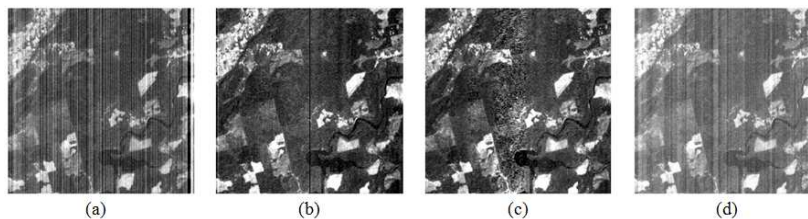


Fig.5: Destriping results of the Hyperion Band 192 (2072.69 nm) image. (a): Original. (b): Destriped by ENVI-SPEAR-Tools – Vertical Stripe Removal. (c): Destriped by the global approach. (d): Destriped by the local approach

6. EVALUATION CRITERIA

To classify the typical ground objects, there is no reliable image reference to compare to the results of classification since the original data are distorted, therefore, we initially made an evaluation of the spectral response of each method and we noted that the global approach yielded the best spectral response, this allowed us to consider the destriping results obtained by the global method as reference data. To evaluate the performance of the destriping algorithms by a supervised classification, we used the PCA for

data reduction, then we constructed the training base by choosing 5 classes, and we applied a supervised classification by the Maximum Likelihood tool of ENVI software. We extracted a training base for the Hyperion datasets of Mt St Helens (USA). In fact, we selected five classes of typical ground objects. These classes are: Dense Vegetation, Bare Soil, Sparse Vegetation, Dense Forest and River Water.

Fig.6 below shows the combinations made on the original data, on the destriped data by ENVI, on the destriped data by the global approach, on the destriped data by the local approach, on the destriped data by the combined wavelet-Fourier filtering and the colored composition of the destriped image by the global approach using 3 exploitable data (3 components) and 7 exploitable (7 components) after data reduction by the PCA of ENVI denoted by PCA 3 and PCA 7 respectively in the rest of the text.

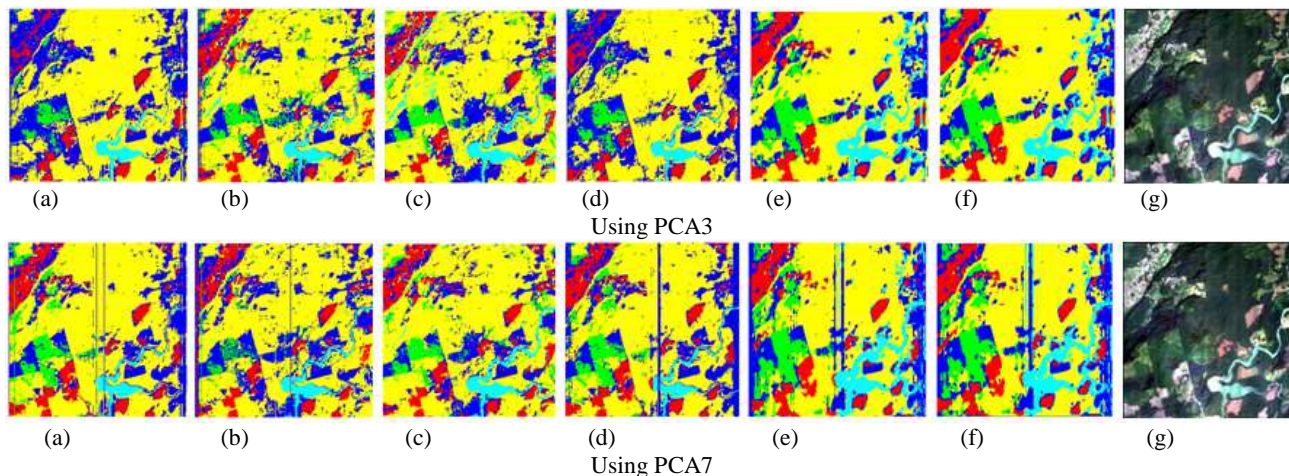
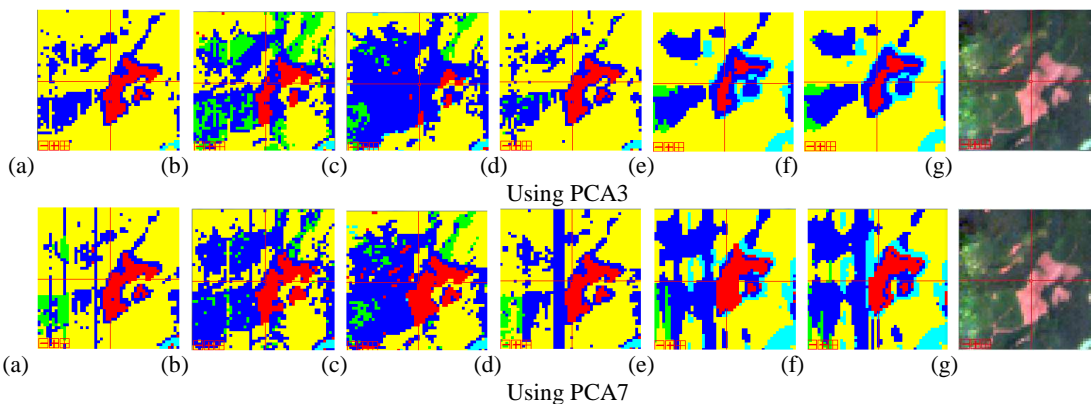


Figure 6. Supervised classification results of the Hyperion datasets of Mt St Helens (USA) after data reduction by the PCA. (a): Original. (b): Destriped by ENVI. (c): Destriped by the global approach. (d): Destriped by the local approach. (e): Destriped by the combined DWT-FFT filtering Level 1. (f): Destriped by the combined DWT-FFT filtering Level 2. (g): The colored composition of the destriped image by the global approach.

In contrast, the best results were collected with the locally calibrated data as it is demonstrated in the zoomed areas illustrated below (Fig.7):

Region 1: R1 (142,150): The best results in Region 1 were obtained using PCA3



Region 2: R2 (48,232): The best results in Region 2 were obtained using PCA3

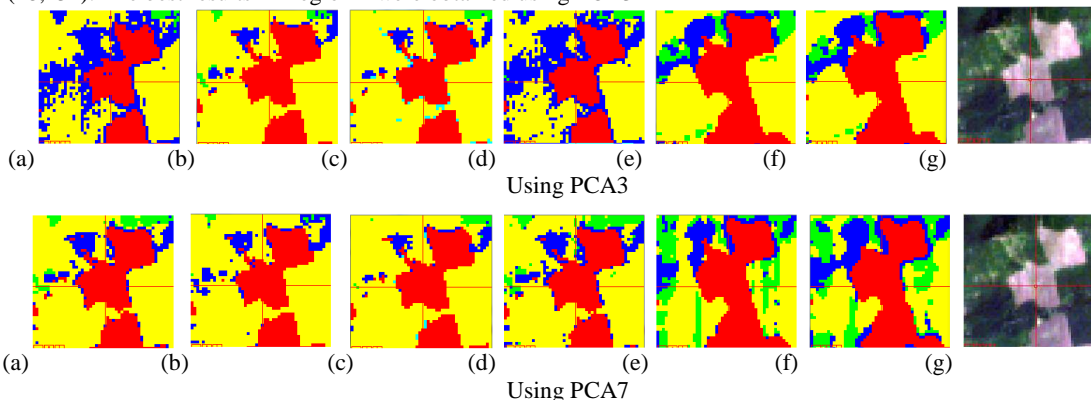


Figure 7. The zoomed areas of the supervised classification results of the position of pixel for the two selected regions. (a): Original. (b): Destriped by ENVI. (c): Destriped by the global approach. (d): Destriped by the local approach. (e): Destriped by the combined DWT-FFT filtering Level 1. (f): Destriped by the combined DWT-FFT filtering Level 2. (g): The colored composition of the destriped image by the global approach.

6. DISCUSSIONS & CONCLUSION

According to the obtained results obtained by the two developed approaches and the one developed by ENVI software, we noticed that the global approach preserves better the spectral features of the typical ground objects since it has the better spectral response than the ENVI and the local destriping methods and has proved its simplicity, high improvement of image quality and efficiency of removing all stripes in the image, but it causes a considerable destruction of the information because it sets the same column mean for all columns.

On the other side, the local approach shows a smoothed calibrated data with some remaining stripes in the band because it recalculates only a small part of the image information which has exceeded the given threshold.

This preprocessing followed by supervised classification. To ensure the reliability of our classification, we used two methods of data reduction which are the PCA of ENVI software and the developed unidimensional wavelet transform applied on the data. The obtained results show that the classification by the local approach characterized better the ground truth than the other methods studied here and the wavelet method showed a better classification than the PCA and confirms that the local approach has the better classification of limits of forests and vegetation than the other methods. Finally, it must also be mentioned that the destriping based on ENVI presents a compromise between the global and local approaches.

REFERENCES

- [1] P.Kawishwar, "Atmospheric Correction Models for Retrievals of Calibrated Spectral Profiles from Hyperion EO-1 Data," Master Thesis of Science in Geo-information Science and Earth Observation, International Institute For Geo-Information Science And Earth Observation, Enschede, The Netherlands,(2007).
- [2] P.Jarecke and K.Yokoyama,"Radiometric calibration of the Hyperion imaging spectrometer instrument from primary standards to end-to-end calibration," Proceedings Optical Science and Technology Symposium, Earth Observing Systems V, SPIE 1435, pp. 1-9,(2000).
- [3] D.X.Kerola, C.J.Bruegge, H.N.Gross and M.C.Helmlinger,"On-Orbit Calibration of the EO-1 Hyperion and Advanced Land Imager (ALI) Sensors Using the LED Spectrometer (LSpec) Automated Facility," IEEE Transactions on Geoscience and Remote Sensing 47(4), pp. 1244-1255,(2009).
- [4] D.L.B.Jupp, "Discussion around Hyperion data," CSIRO Office of Space Science & Applications Earth Observation Centre, Canberra (2001).
- [5] B.Datt and D.L.B.Jupp, "Hyperion Data Processing Workshop, Hands-On Processing Instructions," CSIRO Office of Space Science & Applications Earth Observation Centre, Canberra (2004).
- [6] K.Staenz, R.A.Neville, S.Clavette, R.Landry and H.P.White,"Retrieval of Surface Reflectance from Hyperion Radiance Data," International Geoscience and Remote Sensing Symposium, pp. 1419-1421 (2002).
- [7] W.Kim, "Preprocessing of Hyperion," http://wonkook.com/home/?page_id=196 (2011).
- [8] D.G.Goodenough, A.Dyk, K.O.Niemann, J. S.Pearlman, H.Chen, T.Han, M.Murdoch and C.West,"Processing Hyperion and ALI for forest classification," IEEE Transactions on Geoscience and Remote Sensing 41(6), pp. 1321-1331(2003).
- [9] B.Datt, T.R.McVicar, T.G. Van Niel, D.L.G.Jupp and J.S.Pearlman,"Preprocessing EO-1 Hyperion Hyperspectral Data to Support the Application of Agricultural Indexes," IEEE Transactions on Geoscience and Remote Sensing 41(6), pp. 1246-1259 (2003).
- [10] K.Önder and A.Doğan,"Quantitative and comparative examination of the spectral features characteristics of the surface reflectance information retrieved from the atmospherically corrected images of Hyperion," Journal of Applied Remote Sensing, 7 (1) , 73528 (2013).
- [11] B.Münch, P.Trtik, F.Marone and M.Stampanoni,"Stripe and ring artifact removal with combined wavelet-Fourier filtering," Optics Express, 17(10), pp. 8567-8591(2009).
- [12] J.Chen, Y.Shao, H.Guo, W.Wang and B.Zhu,"Destriping CMODIS Data by Power Filtering," IEEE Trans. Geosci. Remote Sens. 41(9), pp. 2119–2124 (2003).